reactions are produced according to phase space and that the effect of Σ^0 contamination in the Y_1^* peak is negligible.

[9]R. H. Dalitz, Brookhaven National Laboratory Report BNL 735 (T-264) (unpublished).

[10]J. W. Cronin and D. E. Overseth, International Conference on High-Energy Nuclear Physics, Geneva, 1962 (CERN Scientific Information Service, Geneva, Switzerland, 1962), p. 453.

[11]D. Colley et al., Phys. Rev. 128, 1930 (1962).

SPIN AND PARITY OF THE 1385-MeV Y_1^* RESONANCE†

Janice B. Shafer, Joseph J. Murray, and Darrell O. Huwe
Lawrence Radiation Laboratory, University of California, Berkeley, California
(Received 24 January 1963)

Study of the reaction

$$K^- + p \rightarrow Y^{*\pm} + \pi^{\mp} \rightarrow \Lambda + \pi^+ + \pi^- \qquad (1)$$

at a momentum of 1.22 BeV/c has shown conclusively that the spin of the 1385-MeV Y_1^* is $\geq \frac{3}{2}$, as reported earlier by Ely et al.[1]; it has also indicated that the Y_1^* state is $P_{3/2}$ (even $Y^* - \Lambda$ parity) rather than $D_{3/2}$ (odd parity). These conclusions result from the angular distribution of the lambda and the angular dependence of the lambda polarization.

The events were obtained through the use of the 72-inch hydrogen bubble chamber placed in a beam of high-energy K^- mesons extracted from the Bevatron. The momentum spread of the beam was ±2.5%, and the pion background was about 10%.[2]

Approximately 1650 events were analyzed which satisfied the $K^- + p \rightarrow \Lambda + \pi^+ + \pi^-$ hypothesis. Some results from a partial sample were reported earlier.[3] The events were identified by kinematic fitting, first at the decay vertex and then at the production vertex, with the IBM-7090 program "PACKAGE." After this two-step fitting, the number of ambiguous events that might have been $\overline{K}^0$ production rather than lambda production was approximately 1% of the total. Almost complete separation of the $\Sigma^0\pi^+\pi^-$ from the $\Lambda\pi^+\pi^-$ events was accomplished by examination of the ratio $\chi^2(\Lambda\pi\pi)/2\chi^2(\Sigma\pi\pi)$ for each event, the $\Sigma^0\pi\pi$ χ^2 being weighted by a factor of two because of the difference in average χ^2 values. The final $\Lambda\pi^+\pi^-$ sample included about 93% of the true $\Lambda\pi\pi$ events and about 5% of the true $\Sigma^0\pi\pi$ events. The $\Lambda 3\pi$ events were excluded from the $\Lambda\pi\pi$ sample by eliminating all events with $\chi^2(\Lambda 3\pi)$ less than 10.

The cross section for production of the $\Lambda\pi^+\pi^-$ final state by 1.22-BeV/c K^- mesons was determined by comparison with the observed number of tau decays in the same film sample; its value is 2.2 ± 0.2 mb. The angular distributions of Y^{*+} and Y^{*-} production were found similar to that of Y^{*+} production in the work of Ely et al.[1] (see reference 3).

The Dalitz plot for the $\Lambda\pi^-\pi^+$ events is shown in Fig. 1. Projection onto the $\Lambda\pi^+$ mass axis is displayed; the $\Lambda\pi^-$ projection (not shown) is similar. These mass spectra of the $\Lambda\pi^+$ and the $\Lambda\pi^-$ systems are well fitted by Y^{*+} and Y^{*-} resonance curves alone, without background; values of $M(Y^*) = 1385$ MeV and $\Gamma = 50$ MeV are required. The production ratio of Y^{*+} to Y^{*-} is 0.80. Background of 5 to 10% cannot be ruled out.

On the basis of these mass spectra, the limits 1340 MeV $\leq M(Y^*) \leq$ 1430 MeV were utilized in the analysis discussed below. Only events with large production angles in the center of mass

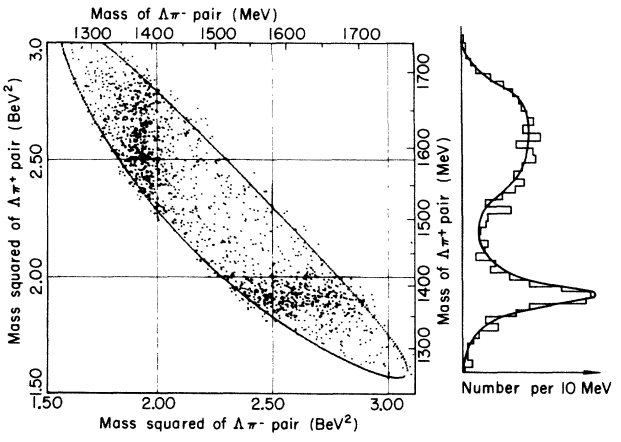

FIG. 1. Dalitz plot of $\Lambda\pi^+\pi^-$ events from K^-p interactions at 1.22 BeV/c. The square of $\Lambda\pi^+$ effective mass is plotted against the square of $\Lambda\pi^-$ effective mass. Scales giving the masses in MeV are also shown. Projection of the events onto the $\Lambda\pi^+$ mass axis is displayed to the right of the figure; the curve represents the fitting of Breit-Wigner resonance expressions to the $\Lambda\pi^+$ and $\Lambda\pi^-$ systems.

were used, because the Y^* polarization was expected to increase with the sine of the production angle. For the study of lambda momentum correlation, only events with $\hat{Y}^* \cdot \hat{K} \leq 0.5$ were included; additional data were required for the polarization study, and events with $\hat{Y}^* \cdot \hat{K} \leq 0.8$ were analyzed.

Angular distribution of lambda.— A particle of spin $\frac{3}{2}$ may decay preferentially along an axis perpendicular to the incident K^- direction, as discussed by Stapp.[4] In this experiment, as well as that of reference 1, the decay of the Y^* was found to produce a correlation between the lambda direction (in the Y^* rest frame) and the production normal [defined as $\hat{n} = (\hat{K} \times \hat{Y}^*)/|\hat{K} \times \hat{Y}^*|$]. Since the Y^{*+} and Y^{*-} distributions were very much alike, the combined data for Y^{*+} and Y^{*-} were used for the $\hat{\Lambda} \cdot \hat{n}$ distribution shown in Fig. 2, with the mass and angle limits specified above. There is no evidence for odd powers of $\hat{\Lambda} \cdot \hat{n}$ in the distribution. The coefficient of the second-order term $(\hat{\Lambda} \cdot \hat{n})^2$ was found to be

$$a_2 = 0.69 \pm 0.22 \quad (2)$$

in a fit of the experimental data to the distribution

$$1 + a_2(\hat{\Lambda} \cdot \hat{n})^2. \quad (3)$$

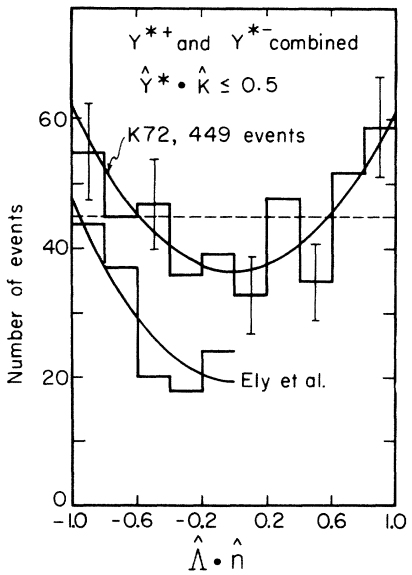

FIG. 2. Lambda angular distribution with respect to the normal to the production plane. The abscissa represents the dot product of a unit vector along the lambda momentum with the unit vector along the normal (in the Y^* rest frame). The data from this experiment (K72) are shown, with a fitted distribution of the form $1 + (0.69 \pm 0.22)(\hat{\Lambda} \cdot \hat{n})^2$. Folded data from reference 1 (Ely et al.) are also shown, with a fitted distribution of the form $1 + (1.5 \pm 0.4)(\hat{\Lambda} \cdot \hat{n})^2$.

This value is to be compared with that found by Ely et al.[1]:

$$a_2 = 1.5 \pm 0.4. \quad (4)$$

The probability that the distribution of Fig. 2 be isotropic was found to be 6%, a value somewhat larger than that of reference 1. Thus spin $\frac{1}{2}$ for the Y^* is not ruled out by the lambda angular distribution presented here.

In comparing with this earlier work of Ely et al., it should be noted that their incident beam momentum was 1.11 BeV/c, appreciably lower than the momentum in this experiment. This could account for larger Y^* polarization. A considerably larger mass band was used for the Y^* events in the former experiment; also various corrections had to be applied to the data. It therefore would not be very surprising if there were a real difference between the two experimental results.

Angular dependence of lambda polarization.— The polarization of the lambda can be expected to give additional information on the spin and also on the parity of the decaying Y^*. The polarization component along a particular axis can be determined by analysis of the pions from lambda decay. The distribution of the pions is of the form

$$1 + \alpha_\Lambda \overline{P}_\Lambda \cdot \hat{p}_\pi = 1 + \alpha_\Lambda [(\overline{P}_\Lambda \cdot \hat{z})(\hat{p}_\pi \cdot \hat{z}) + (\overline{P}_\Lambda \cdot \hat{r})(\hat{p}_\pi \cdot \hat{r})], \quad (5)$$

where $\hat{p}_\pi$ refers to the pion direction in the lambda rest frame, $\hat{z}$ refers to a unit vector along the axis of interest, $\overline{P}_\Lambda \cdot \hat{r}$ is the polarization transverse to $\hat{z}$, and α_Λ is the lambda decay asymmetry with value -0.62. The number of pions going parallel minus the number of pions going antiparallel to this z axis, divided by the total number of pions, is proportional to $\alpha_\Lambda(\overline{P}_\Lambda \cdot \hat{z})$.

In the experiment under discussion, the average value of polarization for the events with $\hat{Y}^* \cdot \hat{K} \leq 0.5$ (and also for $\hat{Y}^* \cdot \hat{K} \leq 0.8$) was close to zero. Along the normal, it was found equal to 0.15 ± 0.08; along the "magic direction" $[\hat{m} = -\hat{n} + 2(\hat{n} \cdot \hat{\Lambda})\hat{\Lambda}]$, the polarization dropped to -0.02 ± 0.08.[5] However, a more detailed study of polarization became possible as the number of measured events increased. For certain values of $\hat{\Lambda} \cdot \hat{n}$, the polarization of the lambda along the normal was found to be almost 60%.

The unnormalized quantity $N_\Lambda \alpha_\Lambda P_\Lambda$ is of more interest than the polarization (or αP_Λ), since the theoretical distributions for the former under various spin-parity assumptions

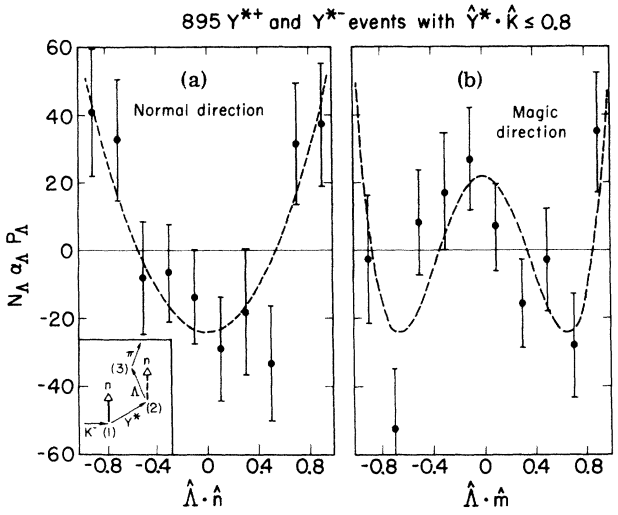

FIG. 3. The components of lambda polarization (multiplied by the number of lambdas and the lambda decay asymmetry) are shown as functions of the lambda direction. The ordinate of Fig. 3(a) represents $N_\Lambda \alpha_\Lambda \times \bar{P}_\Lambda \cdot \hat{n}$ and the ordinate of Fig. 3(b) represents $N_\Lambda \alpha_\Lambda \times \bar{P} \cdot \hat{m}$. The dashed curves represent the best fits [Eq. (6) in the text]. The small sketch in the lower left indicates how successive Lorentz transformations are carried out to find first the Y^* direction in the production center of mass (1), then the Λ direction in the Y^* center of mass (2), and finally the pion direction in the lambda center of mass (3). The lambda momentum and also the lambda polarization are projected onto the normal or the magic direction in the Y^* rest frame (2).

take simple forms. The evaluation of $N_\Lambda \alpha_\Lambda P_\Lambda$, with P_Λ designating a polarization component along a particular axis, is made by finding the sum over all events

$$3 \sum_{i=1}^{N_\Lambda} \cos\theta_i$$

Table I. Lambda polarization.

$\hat{\Lambda}\cdot\hat{n} = \hat{\Lambda}\cdot\hat{m}$	N_Λ	$\bar{P}_\Lambda \cdot \hat{n}$	$\bar{P}_\Lambda \cdot \hat{m}$
-0.9	105	0.58	-0.03
-0.7	99	0.50	-0.78
-0.5	82	-0.15	0.15
-0.3	97	-0.11	0.27
-0.1	69	-0.29	0.58
0.1	82	-0.52	0.15
0.3	78	-0.35	-0.30
0.5	93	-0.53	-0.04
0.7	81	0.59	-0.51
0.9	109	0.51	0.48

(θ_i being defined as the angle between the decay pion and the axis of interest). This quantity is shown in Fig. 3 as a function of lambda momentum projection, both for the normal and the magic directions; i.e., the ordinate of Fig. 3(a) represents $N_\Lambda \alpha_\Lambda \bar{P}_\Lambda \cdot \hat{n}$, and the ordinate of Fig. 3(b) represents $N_\Lambda \alpha_\Lambda \bar{P}_\Lambda \cdot \hat{m}$. The small inset at the lower left in this figure indicates the successive Lorentz transformations which are necessary for the evaluation of the lambda polarization components. Values of polarization components as well as the number of lambdas in each interval are given in Table I.

Fitting with only even terms to the data of Fig. 3 gives the results stated in Table II. (Confidence levels for the best fits improve somewhat with the admixture of small contributions of odd terms.) Figure 3 displays the best-fit curves—a quadratic for the normal distribution and a quartic for the magic-direction distribution. These can be expressed as[6]

$$-1 + 3.5(\hat{\Lambda}\cdot\hat{n})^2 \text{ (normal)}; \qquad (6a)$$

$$1 - 9.7(\hat{\Lambda}\cdot\hat{n})^2 + 11.2(\hat{\Lambda}\cdot\hat{n})^4 \text{ (magic)}. \qquad (6b)$$

Table II. Polarization fits.

Polarization component	Order of fit	Deg of freedom	χ^2	Confidence level	Coefficients 1	$(\hat{\Lambda}\cdot\hat{n})^2$	$(\hat{\Lambda}\cdot\hat{n})^4$
$N_\Lambda \alpha_\Lambda \bar{P}_\Lambda \cdot \hat{n}$	0	4	24.2	7.5×10^{-5}	-0.09 ± 5.2		
	2[a]	3	4.0	0.26	-23.7 ± 7.4	83.0 ± 18.4	
	4	2	4.0	0.13	-23.8 ± 9.1	84.5 ± 66.7	-2.1 ± 81.2
$N_\Lambda \alpha_\Lambda \bar{P}_\Lambda \cdot \hat{m}$	0	4	16.4	0.003	-0.03 ± 4.9		
	2	3	15.3	0.002	5.4 ± 7.1	-19.5 ± 18.2	
	4[a]	2	5.3	0.07	22.0 ± 8.8	-213 ± 64	247 ± 78

[a]Best fits, appropriate for Y_1^* state of $P_{3/2}$.

(For errors on coefficients, see Table II.)

The magic direction has the useful property of yielding maximum polarization for the lambda coming from a certain parent state if the opposite-parity state with the same total spin gives maximum polarization along n. In fact, a more general theorem has been proved for spin $\frac{1}{2}$ and spin $\frac{3}{2}$: Whatever the angular dependence of the polarization component along the normal, the angular dependence of the polarization component along the magic direction is exactly the same for the opposite-parity initial state. The following polarization distributions are obtained for the various Y^* states of interest[6]:

$$\text{for } S_{1/2} \text{ (normal) or } P_{1/2} \text{ (magic)}, \quad 1; \tag{7a}$$

$$\text{for } S_{1/2} \text{ (magic) or } P_{1/2} \text{ (normal)}, \quad -1+2(\hat{\Lambda}\cdot\hat{n})^2; \tag{7b}$$

$$\text{for } P_{3/2}^{\pm 3/2} \text{ (normal) or } D_{3/2}^{\pm 3/2} \text{ (magic)}, \quad 1-(\hat{\Lambda}\cdot\hat{n})^2; \tag{7c}$$

$$\text{for } P_{3/2}^{\pm 1/2} \text{ (normal) or } D_{3/2}^{\pm 1/2} \text{ (magic)}, \quad -1+5(\hat{\Lambda}\cdot\hat{n})^2; \tag{7d}$$

$$\text{for } P_{3/2}^{\pm 3/2} \text{ (magic) or } D_{3/2}^{\pm 3/2} \text{ (normal)}, \quad -1+3(\hat{\Lambda}\cdot\hat{n})^2-2(\hat{\Lambda}\cdot\hat{n})^4; \tag{7e}$$

$$\text{for } P_{3/2}^{\pm 1/2} \text{ (magic) or } D_{3/2}^{\pm 1/2} \text{ (normal)}, \quad 1-15(\hat{\Lambda}\cdot\hat{n})^2+18(\hat{\Lambda}\cdot\hat{n})^4. \tag{7f}$$

(The normal distributions agree with expressions developed earlier by Capps.[7]) The distribution for the magic-direction polarization, $\bar{P}\cdot\hat{m}$, gives additional information over that for the normal polarization, $\bar{P}\cdot\hat{n}$. This is apparent from Eq. (5), the distribution of decay pions; if $\hat{z}$ is defined as the normal, the distribution, in general, has a nonzero $\bar{P}\cdot\hat{r}$ term, which contributes to the magic-direction polarization but not to the normal polarization.

Interpretation of polarization fits.—The assignment of spin $\frac{1}{2}$ for the Y_1^* can be conclusively ruled out by the polarization results (Table II and Fig. 3). Figure 3(a) would have to be isotropic and Fig. 3(b) quadratic if the state were $S_{1/2}$ [see Eqs. (7a) and (7b)]. The situation would be reversed if the state were $P_{1/2}$. Both distributions fit isotropy very badly, with confidence levels of $\leq 10^{-3}$.

Spin $\frac{3}{2}$ is compatible with the polarization data. Further, $P_{3/2}$ is definitely favored over $D_{3/2}$. If a quartic term is added to the expression for 3(a) [in accordance with Eq. (7e)], not only does the confidence level decrease, but the coefficient of the fourth-power term is negligibly small. A second-order fit to 3(b) [Eq. (7d)] is very poor, with a confidence level of 2×10^{-3}. It may be noted also that the coefficients of the best-fit distribution, as given in Eq. (6), agree well in relative sign and in magnitude with the theoretically predicted coefficients for the $P_{3/2}$ decay [Eq. (7)] for an incoherent mixture of $J_z = \pm\frac{1}{2}$ and $J_z = \pm\frac{3}{2}$ states. [The contribution from each of the Eq. (7) distributions is proportional to the difference between the populations of $J_z(+)$ and $J_z(-)$ states. At present it is not clear how interference in decay amplitudes from the different initial states may be expected to affect the polarization distributions.]

Further restriction of polarization fits.—The lambda polarization components along the normal and the magic direction can be analyzed simultaneously. The coefficients of the various powers of $(\hat{\Lambda}\cdot\hat{n})$ or $(\hat{\Lambda}\cdot\hat{m})$ in the two distributions are related for any possible Y^* state by two conditions.

If the Y^* resonance has $L = J - \frac{1}{2}$, the polarization distributions may be written

$$\bar{P}\cdot\hat{n} = A_n^{(0)} + A_n^{(2)}(\hat{\Lambda}\cdot\hat{n})^2 + \cdots + A_n^{(2J-1)}(\hat{\Lambda}\cdot\hat{n})^{(2J-1)},$$

$$\bar{P}\cdot\hat{m} = A_m^{(0)} + A_m^{(2)}(\hat{\Lambda}\cdot\hat{n})^2 + \cdots + A_m^{(2J+1)}(\hat{\Lambda}\cdot\hat{n})^{(2J+1)}.$$

It can be shown that the following relations must always hold:

$$A_n^{(0)} + A_m^{(0)} = 0,$$

$$A_n^{(0)} + A_n^{(2)} + A_n^{(4)} + \cdots + A_n^{(2J-1)} - A_m^{(0)} - A_m^{(2)} - \cdots - A_m^{(2J+1)} = 0.^8$$

Table III. Constrained simultaneous fits of $N_\Lambda \alpha_\Lambda \times P_\Lambda \cdot \hat{n}$ and $N_\Lambda \alpha_\Lambda P_\Lambda \cdot \hat{m}$.

Y^* state	Deg of freedom	χ^2	Confidence level
$S_{1/2}$	9	40.4	6.6×10^{-6}
$P_{1/2}$	9	36.7	3.1×10^{-5}
$P_{3/2}$[a]	7	9.4	0.23
$D_{3/2}$	7	31.9	4.3×10^{-5}
$D_{5/2}$	5	8.3	0.14
$F_{5/2}$	5	8.5	0.13

[a] $P_{3/2}$ fit: for normal, $(-23.0 \pm 5.6) + (81.3 \pm 15.4) \times (\hat{\Lambda} \cdot \hat{n})^2$; for magic, $(23.0 \pm 5.6) + (-220 \pm 46)(\hat{\Lambda} \cdot \hat{n})^2 + (256 \pm 50)(\hat{\Lambda} \cdot \hat{n})^4$.

If the Y^* resonance has $L = J + \frac{1}{2}$, these relations still hold if n and m subscripts are interchanged.

The folded data for the polarization distribution along the normal and the magic direction were simultaneously fitted to the expressions given above, subject to the stated constraints. The distributions and constraints assumed were those appropriate to the Y^* states $S_{1/2}$, $P_{1/2}$, $P_{3/2}$, $D_{3/2}$, $D_{5/2}$, and $F_{5/2}$. The results are given in Table III.

Background and interference effects. —The distributions of Fig. 2 and Fig. 3 have been studied as functions of Y^* mass to determine whether the small background that may be present could influence the results. The value of the $(\hat{\Lambda} \cdot \hat{n})^2$ coefficient for Fig. 2 data is somewhat higher for low-mass than for high-mass Y^*'s; but the coefficients of the normal polarization distribution, Fig. 3(a), are the same within statistics for low-mass and high-mass Y^* events.

The interference of the Y^{*+} and Y^{*-} is small, as shown by the Dalitz plot of Fig. 1 and by the $\hat{\Lambda} \cdot \hat{Y}^*$ plots of reference 3. The latter have slight backward slopes, comparable with those of reference 1.

Conclusions. —The $D_{5/2}$ and $F_{5/2}$ states cannot be ruled out. However, if it is assumed that the spin of the Y^* is most likely $\leq \frac{3}{2}$, the only good fit is that for $P_{3/2}$. As shown in Table III, the constrained fits to polarization data yield a confidence level of 0.23 for the $P_{3/2}$ state; the confidence levels for the other three states with $J \leq \frac{3}{2}$ are all of the order of 10^{-5}. Inspection of the results for separate fits to the normal and magic-direction polarization distributions (Table II) confirms this last conclusion; the conditions stated above which relate to two polarization distributions are considerably better satisfied for the $P_{3/2}$ than for the $D_{3/2}$ state.[9]

The authors wish to acknowledge fruitful conversations with Professor Robert Tripp, who suggested that the magic direction was useful in yielding maximum polarization in a special case of spin-$\frac{3}{2}$ decay, and with Professor Charles Zemach, who has developed the theorem relating parity to interchangeability of normal and magic axes from first principles and shown it to be applicable to any order of spin.

---

†Work done under the auspices of the U. S. Atomic Energy Commission.

[1]R. P. Ely, S. Y. Fung, G. Gidal, Y. L. Pan, W. M. Powell, and H. S. White, Phys. Rev. Letters 7, 461 (1961).

[2]H. K. Ticho, G. Kalbfleisch, J. Kirz, D. Miller, J. B. Shafer, and D. Stork (unpublished).

[3]J. Button-Shafer, D. Huwe, and J. J. Murray, in Prodeedings of the International Conference on High-Energy Nuclear Physics, Geneva, 1962 (CERN Scientific Information Service, Geneva, Switzerland, 1962), p. 303.

[4]H. P. Stapp, Lawrence Radiation Laboratory Report UCRL-9526, 21 December 1960 (unpublished).

[5]As discussed by R. K. Adair, Rev. Modern Phys. 33, 406 (1961), the "magic direction" would be the direction of maximum polarization of the lambda in $P_{1/2}$ decay, while the normal would be the direction of maximum polarization in $S_{1/2}$ decay. Adair has pointed out that $\hat{m}$ can readily be seen to be a direction in the $\hat{n}\hat{\Lambda}$ plane making an angle of $2\theta_{\Lambda n}$ to the normal if one observes that the only operator that can change the parity of the decay, $\bar{\sigma} \cdot \hat{\Lambda}$, is equivalent to a rotation of π about the $\hat{\Lambda}$ axis.

[6]Note that $(\hat{\Lambda} \cdot \hat{m})$ equals $(\hat{\Lambda} \cdot \hat{n})$. If this were not so, the lambda angular distribution of Fig. 2 would depend on the Y^* parity.

[7]Richard H. Capps, Phys. Rev. 122, 929 (1961).

[8]These conditions are most readily found by requiring that $\bar{P} \cdot \hat{m} = \bar{P} \cdot \hat{n}$ for $\hat{\Lambda} \cdot \hat{n}$ or $\hat{\Lambda} \cdot \hat{m} = \pm 1$ $(\hat{m} = \hat{n})$, and $\bar{P} \cdot \hat{m} = -\bar{P} \cdot \hat{n}$ for $\hat{\Lambda} \cdot \hat{n}$ or $\hat{\Lambda} \cdot \hat{m} = 0$ $(\hat{m} = -\hat{n})$.

[9]Work has recently been reported which gave indication (two standard deviations) of $P_{3/2}$ as the Y^* state if the spin of $\frac{3}{2}$ were assumed. The final state, from $\pi^- p$ interactions, was complicated by the presence of the K^* resonance (37%); D. Colley, N. Gelfand, U. Nauenberg, J. Steinberger, S. Wolf, H. R. Brugger, P. R. Kramer, and R. J. Plano, Phys. Rev. 128, 1930 (1962).